Influence of ground improvement on the surface response of liquefiable ground

C.Y. Han & R.P. Orense

University of Auckland, Auckland, New Zealand

2013 NZSEE Conference

ABSTRACT: The Christchurch earthquakes have shown that liquefaction and associated ground deformations are major hazards to the built environment. To prevent the occurrence of liquefaction, ground improvement techniques, such as densification or solidification, are usually implemented at potentially liquefiable sites. However, current practice does not consider the effect of the change in ground stiffness resulting from improvement works on the overall seismic response of the sites. In this paper, ground improvement method was implemented to three different types of liquefiable model ground by changing the shear wave velocities of the liquefiable layers to values which are sufficient to prevent the occurrence of liquefaction. Then, 1D total stress and effective stress analyses were conducted using three different base input motions with varying amplitudes to estimate the seismic response at the ground surface. Based on the results considering different model grounds, input base motions and maximum amplitudes, the general trend observed was an increase in peak ground acceleration (PGA) in improved grounds when compared to the unimproved ones. The findings indicate the importance of considering the effect of remediating liquefiable grounds on the surface PGAs as this may have serious effects on the buildings built on top of them.

1 INTRODUCTION

Liquefaction of loose saturated sandy grounds during earthquakes often causes damage to structures, for example, through the settlement of buildings caused by the loss of soil strength. In Christchurch, for example, several buildings sank and tilted as a result of the extensive liquefaction in the area caused by the 2010-2011 earthquake sequence (Orense et al. 2011), as shown in Figure 1. Other recent large-scale earthquakes, such as the 2011 off the Pacific Coast of Tohoku Earthquake in Japan, showed that buildings and other civil engineering structures are vulnerable to liquefaction-induced damage (Orense et al. 2012).

Currently, several remedial measures are available in treating or improving sites susceptible to soil liquefaction. The most popular measure involves improving the liquefiable soil so that liquefaction will not occur; these include densification and solidification methods. In selecting the appropriate remedial measures, various factors, such as effectiveness of improvement, required areas and depth of improvement, effects on surrounding environment, cost and ease of execution, and level of desired improvement to name a few, should be considered.

When improving liquefiable layers, the effect of possible ground motion amplification is not usually considered in the design. Due to the increase in stiffness, the improved ground may result in increase in ground motion, and this may be detrimental to the structure on top of it. Although little information is available regarding the influence of size of improved ground and its stiffness on ground motions, engineers should consider a balance in design such that the size and stiffness of the improved ground would result in acceptable deformations and accelerations of the structure during an earthquake.

This paper investigates the effect of increased stiffness of the remediated layers on the surface ground motion through 1D seismic response analyses. For this purpose, three different 1D soil profiles were considered and subjected to different base excitations. The results highlight the need to incorporate the change in soil stiffness in the design of remediation techniques for liquefiable sites.

Figure 1: Differential settlement and tilting of structures during the 2011 Christchurch earthquake.

2 DESCRIPTION OF MODEL GROUNDS AND INPUT MOTIONS

In this study, several series of one-dimensional seismic response analyses were performed using the computer program DEEPSOIL (Hashash 2008). In the analyses, the ground models shown in Figure 2 are employed. These three profiles, which are representative of sites in Christchurch, have natural periods ranging from T_g=0.22 to 0.61 sec. The shear wave velocities indicated in the figure were estimated from available data. Engineering bedrock is taken as the layer with shear wave velocity V_S=400 m/s, as usually employed in practice.

The dynamic characteristics of each layer in the soil profile (i.e. strain-dependency of modulus and damping) were estimated from relations recommended by various researchers (e.g., Seed and Idriss 1971). The soil curves were defined using the Modified Reduction Factor (MRDF) pressure-dependent hyperbolic model developed by Dobry (1985). For the effective stress analysis, the constitutive model formulated by Matasovic and Vucetic (1993) was used. Table 1 lists the parameters used in the analysis. Details of these parameters are provided in the appropriate references.

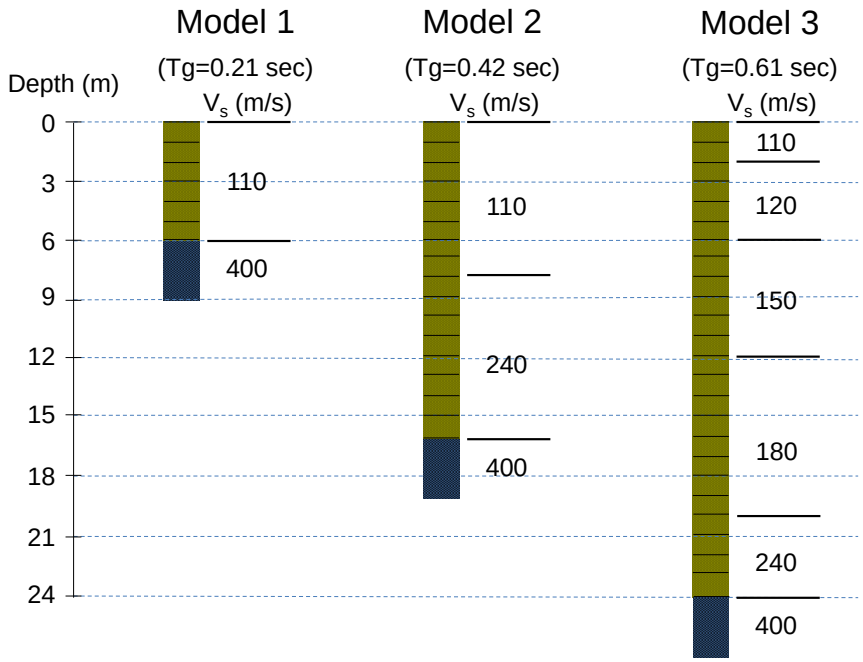

Figure 2: Model grounds used in the analysis.

Table 1: Input parameters used in the analyses

Total stress analysis		**Effective stress analysis**		
Model parameter	Value	Model parameter	Unimproved ground	Improved ground
Reference Strain (%)	0.061	PWP Model	1	1
Reference Stress (MPa)	0.18	f	1	1
Stress-strain curve parameter, β	1.455	p	1.15	1.15
Stress-strain curve parameter, s	0.855	F	V_s = 110 – 120 → F = 4.35 V_s = 150 – 180 → F = 3.25 V_s = 110 – 120 → F = 2.25	4.35
Pressure-dependent parameter, b	0	s	0.4	0.4
Pressure-dependent parameter, d	0	γ (threshold strain value)	0.02	1
MRDF Parameter, P_1	0.992	v	3.8	3.8
MRDF Parameter, P_2	0.380			
MRDF Parameter, P_3	1.195			

Three strong motion records were used as input motion (E+F) at the bedrock. These include (1) Site 033C (Dannevirke Post Office) S23E motion recorded during the 1990 Weber 2 earthquake (with predominant period, i.e., period at which the maximum spectral acceleration occurs in an acceleration response spectrum calculated at 5% damping, of T_p=0.10 sec); (2) CHCH (Christchurch Hospital) N01W motion recorded during the 2011 Christchurch earthquake (T_p=0.24 sec); and (3) an artificial motion based on Japanese Design Spectra (JDS) for soft soil (T_p=1.28 sec). The time histories of these acceleration records and the corresponding Fourier spectra are illustrated in Figure 3. Both low-pass and high-pass filters were used in the analysis. Moreover, two levels of maximum amplitude of bedrock input motion were used: 0.1g and 0.3g.

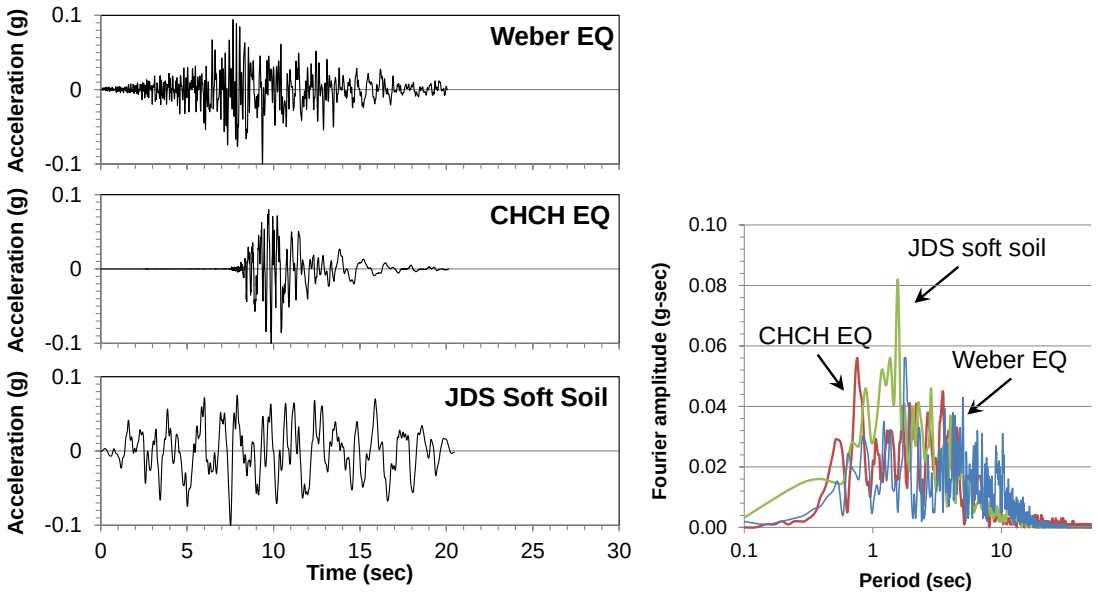

Figure 3: Strong motion records used in the analysis and corresponding Fourier spectra (normalised to 0.1g maximum)

3 ANALYSES CONDUCTED AND DISCUSSION OF RESULTS

3.1 Computer Program Used

In the seismic response analyses, the computer program DEEPSOIL was used. DEEPSOIL is a one-dimensional site response program that performs analyses in the frequency- (linear and equivalent linear) and in the time- (linear and nonlinear) domain. The code has a graphical user-interface that allows for the selection of modes/frequencies of viscous damping formulation and nonlinear soil parameters. The modified hyperbolic model (Hashash and Park 2001) implemented in the code permits accounting for stress and strain dependencies of the soil behaviour by means of an appropriate definition of the model parameters that can be done by using a fitting curve procedure which is fully automated in the program. The 1-D time domain analyses are performed to solve the dynamic equations of the motion on a lumped mass scheme. For saturated subsoils, the program also allows conducting wave propagation analysis with pore water pressure generation and dissipation. In this paper, DEEPSOIL v.4.0 was used.

3.2 Method of analysis

3.2.1 *Total and effective stress analysis*

In the first stage of the analysis, each of the assumed model ground profile was analysed using the seismic input motions mentioned in the preceding section, with peak values of 0.1g and 0.3g. Both total stress analysis and effective stress analysis were performed considering each of the 18 scenarios (3 model grounds, 3 input motions and 2 levels of PGA).

3.2.2 *Liquefaction potential evaluation*

Next, based on the results of total stress analyses, the layers which will liquefy were identified. These were done by calculating the Factor of Safety against Liquefaction, F_L, for each layer of the model ground. The factor of safety F_L against liquefaction is defined by:

$$F_L = \frac{CRR}{CSR} \tag{1}$$

where *CRR* is the cyclic resistance ratio and *CSR* is the cyclic shear stress ratio induced by the earthquake. *CRR* was read from the empirical chart proposed by Andrus and Stokoe (1997) based on the following relationship between *CRR* and V_s:

$$CRR = a\left(\frac{V_{s1}}{100}\right)^2 + b\left(\frac{1}{V_{s1}^* - V_{s1}} - \frac{1}{V_{s1}^*}\right) \tag{2}$$

where a and b are fitting parameters, and V^*_{s1} is the limiting (upper) value of V_s for liquefaction occurrence. From the "best fit" curve by Tokimatsu and Uchida (1990), V^*_{s1} is chosen to have a value of 210 m/sec. Note that V_{s1} is the overburden stress-corrected shear wave velocity as proposed by various researchers (e.g. Sykora 1987). It was assumed that the earthquake has *M*7.5. On the other hand, the *CSR* at a particular depth of a soil deposit can be expressed as:

$$CSR = \frac{\tau_{ave}}{\sigma'_{v0}} = \frac{0.65 \times \tau_{\max}}{\sigma'_{v0}} \tag{3}$$

Where σ'_{v0} is the effective vertical overburden stress at the target depth in soil profile, and τ_{ave} is the average cyclic shear stress caused by the earthquake and is assumed to be 0.65 of the maximum induced stress $\tau_{\max}$. The value of $\tau_{\max}$ is obtained from the results of the total stress analysis.

3.2.3 *Required level of ground improvement to mitigate liquefaction*

For layers that will liquefy (F_L<1.0), the corresponding shear wave velocity was increased incrementally in order for liquefaction not to occur at that layer. The step-by-step procedure adopted was as follows:

(1) Using the original shear wave velocities of the soil profile, calculate the maximum shear stress through total stress analysis (using DEEPSOIL), and evaluate F_L using Eqtn (1).
(2) Determine the layer(s) which will liquefy (i.e. $F_L < 1$)
(3) For liquefiable layers, increase the value of V_s to achieve $F_L \geq 1$. Note that when V_s is increased, the corresponding *CRR* also changes.
(4) Run the total stress analysis again, this time using the new V_s.
(5) Check if the new V_s for the layer will generate an F_L value close to but greater than 1.0.
(6) Repeat step (3) until all layers show $F_L \geq 1$.

Note that each soil profile responds differently when subject to different seismic motions and the required V_s for each sub-layer may not be the same for all input motions. Thus, trial-and-error procedure was used to obtain the most appropriate V_s which would represent the improved ground. The new sets of V_s for the improved grounds are listed in Tables 2 – 4. The green zones are the sub-layers which experienced liquefaction and therefore new V_s were assigned. The orange blocks are the sub-layers that initially did not liquefy, but were forced to be changed to achieve $F_L \geq 1$; these layers became liquefiable as a result of changes in the stiffness of other sub-layers. As expected, the required V_s to sustain 0.3g input motions are greater than those needed for 0.1g input motions.

Table 2: Shear wave velocity for the improved ground (Ground Model 1)

Layer	Original V_s (m/s)	Adjusted V_s for $F_L \geq 1$ (m/s)					
		0.1g CHCH EQ	0.1g JDS	0.1g Weber EQ	0.3g CHCH EQ	0.3g JDS	0.3g Weber EQ
1	110	110	110	110	110	110	110
2	110	130	110	120	140	140	140
3	110	140	130	140	150	150	150
4	110	150	140	150	160	160	160
5	110	160	150	150	170	170	170
6	110	160	160	160	175	175	175

Table 3: Shear wave velocity for the improved ground (Ground Model 2)

Layer	Original V_s (m/s)	Adjusted V_s for $F_L \geq 1$ (m/s)					
		0.1g CHCH EQ	0.1g JDS	0.1g Weber EQ	0.3g CHCH EQ	0.3g JDS	0.3g Weber EQ
1	110	110	110	110	110	110	110
2	110	120	120	120	140	140	140
3	110	140	130	130	150	150	150
4	110	150	140	140	160	160	160
5	110	150	150	150	170	170	170
6	110	160	160	150	175	175	170
7	110	160	170	150	180	180	180
8	110	160	170	160	190	190	180
9	240	240	240	240	240	240	240
10	240	240	240	240	240	240	240
11	240	240	240	240	240	240	240
12	240	240	240	240	240	240	240
13	240	240	240	240	240	240	240
14	240	240	240	240	240	240	240
15	240	240	240	240	240	240	240
16	240	240	240	240	240	240	240

Table 4: Shear wave velocity for the improved ground (Ground Model 3)

Layer	Original V_s (m/s)	Adjusted V_s for $F_L \geq 1$ (m/s)					
		0.1g CHCH EQ	0.1g JDS	0.1g Weber EQ	0.3g CHCH EQ	0.3g JDS EQ	0.3g Weber EQ
1	110	110	110	110	110	110	110
2	110	110	120	110	130	140	130
3	120	130	130	120	140	150	140
4	120	130	140	130	150	160	150
5	120	140	150	130	160	170	160
6	120	140	160	140	170	170	170
7	150	150	160	150	170	180	170
8	150	150	170	150	180	190	170
9	150	150	170	150	180	190	180
10	150	160	180	150	190	200	180
11	150	160	180	150	190	200	180
12	150	160	180	150	190	200	190
13	180	180	190	180	200	210	190
14	180	180	190	180	200	210	190
15	180	180	190	180	200	210	190
16	180	180	190	180	210	220	200
17	180	180	190	180	210	220	200
18	180	180	190	180	210	220	200
19	180	180	190	180	210	220	200
20	180	180	200	180	210	230	200
21	240	240	240	240	240	240	240
22	240	240	240	240	240	240	240
23	240	240	240	240	240	240	240
24	240	240	240	240	240	240	240

3.2.4 *Comparison of acceleration profiles between improved and unimproved grounds*

Comparisons of the maximum acceleration (PGA) distribution for the three soil profiles without improvement (original V_s) and with ground improvement (new V_s) are shown in Figures 4 and 5 (for Model 1 and 3, respectively), when subjected to the specified base motions with maximum amplitude of 0.1g and 0.3g. It can be seen in the plots for 0.1g that, regardless of the input motion used, the PGA profiles were generally similar for both unimproved and improved grounds. The surface PGAs for the improved ground appear to be larger for the shallower soil model, but as the depth of the soft deposit increases, the difference in surface PGA becomes negligible.

On the other hand, the difference in surface PGA becomes remarkable when the soil layers were subjected to higher amplitude of input motion (i.e. 0.3g). The surface PGA values of improved ground are higher by about 30% to almost twice those of the unimproved ground. Thus, the amplification of motion due to the increase in stiffness becomes more pronounced with the increase in amplitude of the base motion.

3.2.5 *Results of effective stress analyses*

Effective stress analyses were also performed on the model grounds; however, due to space limitation only the results for Model 3 at 0.3g are presented herein (see Figure 6). The PGA distributions for the unimproved grounds generally were lesser than those obtained from total stress analysis, as the soil softening (due to the build-up of excess pore pressure) attenuates the motion as it propagates from the

bottom to the top of the deposit. Needless to say, the results of both total and effective stress analyses for the improved grounds were generally similar, since liquefaction was not allowed to occur. Comparing the seismic response at the surface of improved and unimproved grounds using effective stress analyses, the surface PGAs of improved grounds were between 2-3 times more than those of the unimproved grounds. It is worth mentioning that layers which developed high excess pore water pressure matched very well with layers deemed to have liquefied in the total stress analysis (F_L<1).

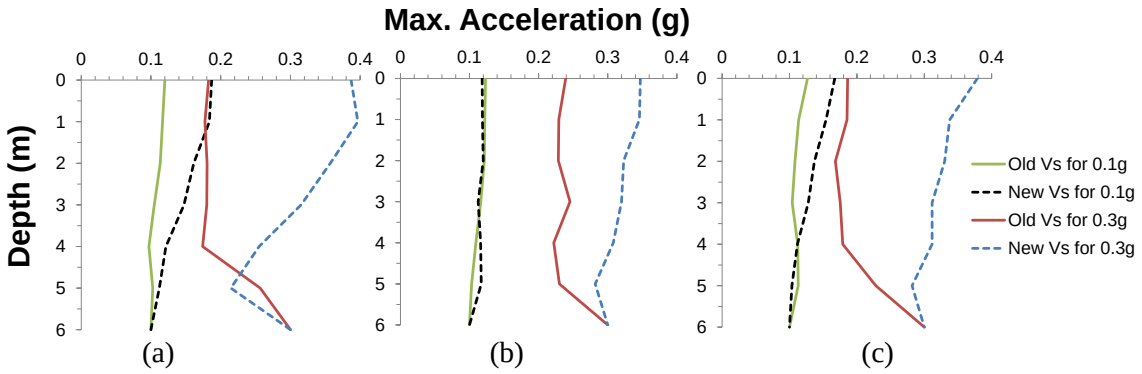

Figure 4: Comparisons of PGA profiles from total stress analysis for Ground Model 1 (6m deep) when subjected to 0.1g and 0.3g: (a) CHCH EQ; (b) Soft soil JDS; and (c) Weber EQ motion.

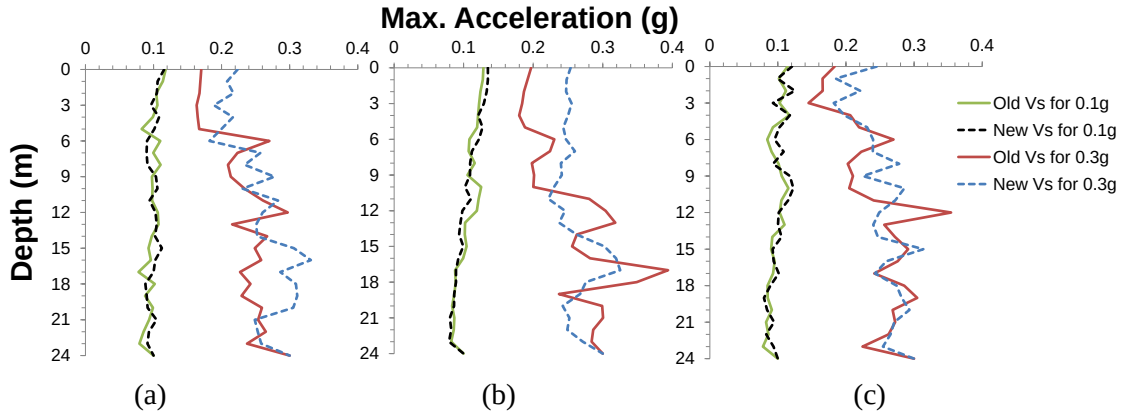

Figure 5: Comparisons of PGA profiles from total stress analysis for Ground Model 3 (24m deep) when subjected to 0.1g and 0.3g: (a) CHCH EQ; (b) Soft soil JDS; and (c) Weber EQ motion.

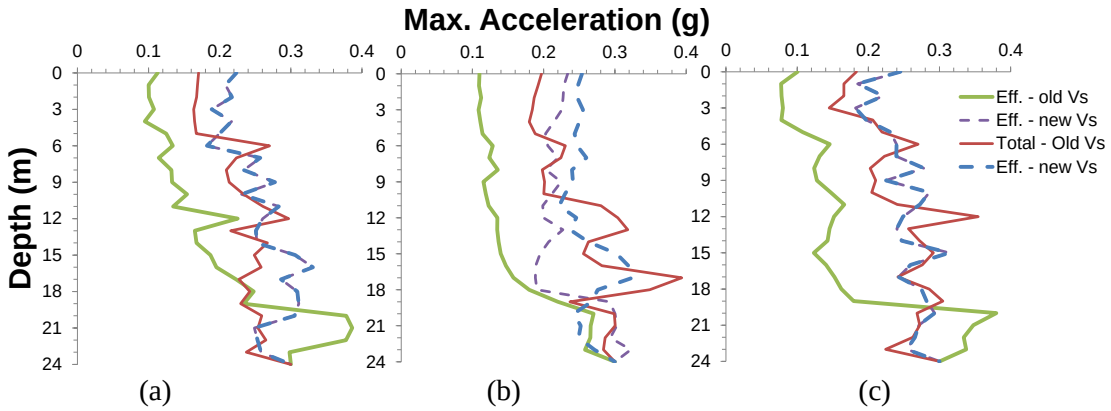

Figure 6: Comparisons of PGA profiles from total and effective stress analysis for Ground Model 3 (24m deep) when subjected to 0.3g: (a) CHCH EQ; (b) Soft soil JDS; and (c) Weber EQ motion.

4 CONCLUSIONS

In this paper, the effect of increased soil stiffness due to ground improvement work as liquefaction countermeasure on the seismic response of the deposit was investigated. For this purpose, three model grounds, three acceleration time histories and two amplitudes of motions were used. The following are the major conclusions observed:

1. The required soil stiffness to prevent liquefaction can be determined from total stress analysis using one-dimensional seismic response calculation. Due to changes in soil stiffness, the shear wave velocity of some layers which initially were deemed not to liquefy needed to be increased to maintain $F_L \geq 1.0$ condition.
2. The results of total stress analysis showed that when the amplitude of base motion was low (0.1g), the surface PGAs of the improved ground were not much different to those of unimproved ground especially when the soft deposit was deep. On the other hand, when the amplitude of base motion was high (0.3g), the amplification of PGA was very pronounced, with the surface PGAs in improved grounds between 2-3 times higher than those of unimproved ones.
3. The results of effective stress analyses showed more significant difference between the surface PGAs of improved and unimproved grounds.

Although the cases considered herein may not have captured all possible range of soil profiles and input motions, the results of the study highlighted the need to incorporate the change in soil stiffness in the design of remediation techniques for liquefiable sites.

REFERENCES:

Andrus, R. D. and Stokoe, K. H. I. 1997. Liquefaction resistance based on shear wave velocity. *Proc., NCEER Workshop on Evaluation of Liquefaction Resistance of Soils*, Nat. Ctr. for Earthquake Engrg. Res., State Univ. of New York at Buffalo: 89-128.

Dobry, R. 1985. Pore pressure model for cyclic straining of sand. *Research Report*, Civil Engineering Department, Rensselaer Polytechnic Institute, Troy, NY 12180, USA.

Hashash Y.M.A. and Groholski, D.R.D. 2008. *DEEPSOIL v4.0beta: User Manual and Tutorial*. pp. 98.

Hashash, Y. M. A. and Park, D. 2001. Non-linear one-dimensional seismic ground motion propagation in the Mississippi embayment. *Engineering Geology* 62 (1-3): 185-206.

Matasovic, N. and Vucetic, M. 1993. Cyclic characterization of liquefiable sands. *Journal of Geotechnical Engineering*, ASCE 119 (11): 1805-1822.

Orense, R.P., Kiyota, T., Yamada, S., Cubrinovski, M., Hosono, Y., Okamura, M., Yasuda, S. 2011. Comparative study of liquefaction features observed during the 2010 and 2011 Canterbury earthquakes. *Seismological Research Letters*, Vol. 82, No. 6, 905-918.

Orense, R., Yamada, S. and Otsubo, M. 2012. Soil liquefaction in Tokyo Bay Area due to the 2011 Tohoku (Japan) Earthquake. *Bulletin of the New Zealand Society for Earthquake Engineering*, Vol. 45, No. 1, March Issue, 15-22

Seed, H. B. and Idriss, I.M. 1971. Simplified procedure for evaluating soil liquefaction potential. *ASCE J Soil Mech Found Div* 97 (SM9): 1249-1273.

Sykora, D. W. 1987. Creation of a data base of seismic shear wave velocities for correlation analysis. *Geotech. Lab. Misc. Paper GL-87-26*, U.S. Army Engr. Waterways Experiment Station, Vicksburg, Miss.

Tokimatsu, K. and Uchida, A. 1990. Correlation between liquefaction resistance and shear wave velocity. *Soils and Foundations* 30 (2): 33-42.